Computation of heats of transport in crystalline solids: II

2008 J. Phys.: Condens. Matter 20 425201

(http://iopscience.iop.org/0953-8984/20/42/425201)

J. Phys.: Condens. Matter **20** (2008) 425201 (7pp) doi:10.1088/0953-8984/20/42/425201

Computation of heats of transport in crystalline solids: II

P J Grout[1] **and A B Lidiard**[2]

[1] The Department of Chemistry, Physical and Theoretical Chemistry Laboratory, University of Oxford, South Parks Road, Oxford OX1 3QZ, UK
[2] The J J Thomson Physical Laboratory, University of Reading, Whiteknights, Reading RG6 6AF, UK

E-mail: Peter.Grout@chem.ox.ac.uk

Received 9 May 2008, in final form 21 July 2008
Published 9 September 2008
Online at stacks.iop.org/JPhysCM/20/425201

Abstract

This paper explores the application of classical molecular dynamics to the computation of the heat of transport of Au atoms in a model of solid gold at several elevated temperatures above the Debye temperature. It is assumed that the solid shows vacancy disorder. The work shows that to obtain consistent and reliable results it is necessary (a) to use very small time steps ($\approx$1 fs) in the molecular dynamics integration routine and (b) to take averages over a very large number of vacancy displacements—a number which varies with temperature but which is of the order of 10^5.

The results for the reduced heat of transport for the Au atoms show that: (1) it is positive in sign, i.e. that the diffusion of Au atoms in a temperature gradient is biassed towards the cold region or equivalently that the vacancies tend to migrate towards the hotter region; (2) it is predicted to fall as the average temperature increases and that the variation is closely linear in $(1/T)$; (3) its value at high T relative to the energy of activation for vacancy movement is close to the corresponding ratio of experimental quantities. Analysis of these results indicates that the method and model may allow reliable predictions for other metals having the face centred cubic structure.

1. Introduction

The phenomenology of atomic transport in a temperature gradient is subject to a number of minor variations. Here we shall use a description which is based on the thermodynamics of irreversible processes (see, for example, Allnatt and Lidiard 1993, Flynn 1972, Philibert 1991, Shewmon 1989). In this the effect of the temperature gradient on the migration of atoms is characterized by a parameter called the heat of transport, often denoted by Q^*. For example, in the simplest case the flux of a species in a solution, fluid or solid, is given by

$$\mathbf{J}_k = -L_k \left[T\nabla\left(\frac{\mu_k}{T}\right) + \frac{Q_k^* \nabla T}{T} \right] \tag{1}$$

in which μ_k is the chemical potential of the species k and Q_k^* is the corresponding heat of transport. It is often convenient to work instead with the alternative, but equivalent, expression

$$\mathbf{J}_k = -L_k \left[(\nabla\mu_k)_T + \left(Q_k^* - h_k\right)\frac{\nabla T}{T} \right] \tag{2}$$

in which $(\nabla\mu_k)_T$ denotes that part of the gradient of chemical potential due to gradients in pressure and concentration but not temperature. The quantity $Q_k^{*\prime}$ given by

$$Q_k^{*\prime} = Q_k^* - h_k \tag{3}$$

where h_k is the partial enthalpy of k is called the reduced heat of transport (see e.g. Allnatt and Lidiard 1993). These heat of transport parameters determine effects such as thermodiffusion, the Ludwig–Soret effect in solutions and thermoelectric effects in ionic conductors. Such effects can be of substantial importance in various experimental and practical situations, while experimental studies have been conducted on metals, alloys and ionic crystals (see e.g. Allnatt and Chadwick 1967, Wever *et al* 1973, Janek *et al* 2002). In general, atomic transport in solids has been well interpreted in terms of the theory of mobile point defects—vacancies and interstitials—in these systems, so the theoretical problem reduces to that of understanding the heats of transport of the relevant mobile defects.

The calculation of heats of transport in terms of other properties of the systems of interest has therefore long presented a challenge to theorists. Although there have been many discussions of this problem over the years and some salient features may have been identified, little real progress towards a predictive, quantitative theory for solids can be said to have been made until recent years. In particular, the understanding of the heat of transport of defects in terms of interatomic interactions bears no comparison with the calculation of other defect properties in solids (see, for example, Harding 1990 and Doan 1988). However, an approach proposed originally by Gillan and Finnis (1978) and by Gillan (1983), but limited to 0 K, was extended later to non-zero temperatures by Jones *et al* (1996, 1997, 1999) who made a series of calculations for vacancies by means of molecular dynamics simulations, mainly of a Lennard-Jones model of solid Ar. That system was chosen in view of previously published work on the properties of vacancies in it which allowed important checks on the accuracy of the calculations (Becker and Hoheisel 1982 and Vogelsang and Hoheisel 1986, 1987a, 1987b). This work led to a number of general conclusions, one of which was the temperature dependence of the vacancy heat of transport.

The present paper is a continuation of that work but carried out on an interatomic potential model of Au. There are several reasons for this choice. One is that several experimental measurements of the vacancy heat of transport in Au have been made and are in substantial agreement with one another (Jaffe and Shewmon 1964, Meechan and Lehman 1962 and Mock 1969). A second is that estimates of the electronic contribution to Q^* by the method of Gerl (1967) indicated it to be relatively small (see also Wever *et al* 1973). We are therefore here concerned only with the contribution from atomic movements. Our approach is essentially the same as that described in detail in the previous paper (Jones *et al* 1999) and we therefore refer the reader to that for a full description of the basic computational method. However, to avoid any confusion we note here that our method, since it derives from the Green–Kubo approach to the calculation of transport coefficients from averages of time–correlation functions in a system in thermal equilibrium, uses isothermal molecular dynamics, not non-equilibrium molecular dynamics (NEMD), sometimes used for analogous problems in fluids (see e.g. Hoheisel and Vogelsang 1988). As proposed by Gillan and Finnis (1978) and analysed more fully by Allnatt (2001) we can obtain the heat of transport, Q_k^* from the isothermal relation

$$\mathbf{J}_q = Q_k^* \mathbf{J}_k \tag{4}$$

by representing the matter flux of species k, $\mathbf{J}_k$, in terms of discrete atomic jumps and by obtaining the accompanying heat flux, $\mathbf{J}_q$, by molecular dynamics. This proposal was made feasible by a device for handling rare, thermally activated events in molecular dynamics which had been suggested earlier by Bennett (1975) and used subsequently in other applications (e.g. Gillan *et al* 1987). The macroscopic heat current is then obtained by averaging the corresponding atomic dynamical variable, which for atoms interacting via a central pairwise potential is (Irving and Kirkwood 1950)

$$\mathbf{J}_q(t) = \sum_i \left(\tfrac{1}{2} m_i v_i^2 \mathbf{I} + \tfrac{1}{2} \sum_{j \neq i} \left[\phi\left(\mathbf{r}_i - \mathbf{r}_j\right) \mathbf{I} - \frac{\left(\mathbf{r}_i - \mathbf{r}_j\right)\left(\mathbf{r}_i - \mathbf{r}_j\right)}{\left|\mathbf{r}_i - \mathbf{r}_j\right|} \frac{\partial \phi\left(\left|\mathbf{r}_i - \mathbf{r}_j\right|\right)}{\partial r_i} \right] \right) \cdot \mathbf{v}_i \tag{5}$$

in which $\mathbf{r}_i$ and $\mathbf{v}_i$ are the position and velocity of the atom i, $\mathbf{I}$ is the unit tensor and $\phi(|\mathbf{r}_i - \mathbf{r}_j|)$ is the central interatomic potential of the interaction of atoms i and j. As we see, this heat current is made up of three terms: the first is a current of kinetic energy, the second is a current of potential energy and the third is a current of a virial of the forces (although this tensor quantity is not the usual virial of Clausius). This third term can also be regarded as a current of energy deriving from the work done on atoms i by the movements of atoms j since the Cartesian tensor quantity

$$\sigma_j^{\alpha\beta} \equiv \frac{1}{2v_\mathrm{a}} \sum_{i \neq j} \frac{(\mathbf{r}_i - \mathbf{r}_j)^\alpha (\mathbf{r}_i - \mathbf{r}_j)^\beta}{|\mathbf{r}_i - \mathbf{r}_j|} \frac{\partial \phi(|\mathbf{r}_i - \mathbf{r}_j|)}{\partial r_i}$$

may be used to represent the $\alpha\beta$-component of the local stress at the position of atom j (see e.g. Born and Huang (1954), especially section 11). (Here v_a is the volume per atom.) This term proves generally to be the computationally intensive part of the calculated current.

The important quantity is then the average heat current in the direction of the atom jump, i.e.

$$\overline{q}(t) = \left\langle \mathbf{e}_0 \cdot \mathbf{J}_q\,(t) \right\rangle \tag{6}$$

in which $\mathbf{e}_0$ is the unit vector in the jump direction, i.e. $\frac{1}{\sqrt{2}}(1, 1, 0)$ for movements between nearest neighbour sites in the fcc lattice. The angular brackets denote an average over all *successful* jumps of the atom into the vacant site, i.e. over all trajectories of the system leading to a net displacement in the defined hopping direction. (For the circumstances of the present calculations the unsuccessful jumps amount to about 15% of the total.) Thus $\overline{q}(t)$ is the average heat current per single atom jump at time t after the atom passes through the transition state. Finally, the heat of transport of the atom jumping into the vacancy, as derived by Gillan (1977), is

$$Q_\mathrm{G}^* = \frac{2}{s} \int_0^\infty q\,(t)\,\mathrm{d}t \tag{7}$$

in which s is the jump distance, i.e. the nearest neighbour separation. The corresponding value for the vacancies is the negative of (7). This relation provides the basis for the computations reported here.

The plan of this paper is as follows. In the next section we describe a number of other details relating to these calculations This section also emphasizes that the heat flow directly given by the method of Gillan and Finnis (1978) is relative to the centre of mass of the solid and that this has to be corrected to give the required flow relative to the crystal lattice. Section 3 describes our results further and section 4 gives our conclusions.

2. The present calculations

The broad objectives of our work are twofold. One is to obtain guidance on the dependence of Q^* upon physical parameters, such as pressure, temperature, lattice structure, interatomic forces, etc. However, previous work, both published and unpublished, has indicated that some of the results can be sensitive to certain unavoidable artefacts of the method, e.g. the number of distinct trajectories to obtain the necessary averages over defect jumps, the time step used in the integration of the equations of motion of the atoms in the solid, the size of the periodicity volume, etc. A second objective is to remove such inaccuracies and uncertainties in the method. The present paper therefore sets out to describe our understanding of the method by obtaining accurate results against a small number of variables. At the same time we shall compare our predictions against the known experimental results for Au.

In this section we first describe the potential energy function of the physical model and then some aspects of the computation of the heat of transport. As the atomic model we chose a two-body potential model of Au due to Cherns *et al* (1977) and Gillan and Finnis (1978), which is a modified Morse potential originally constructed to represent the sputtering of Au atoms by high energy ion beams (see the appendix). Its *form*, i.e. its short range and simple two-body character is advantageous for our purposes partly because it avoids the relatively long tail of the Lennard-Jones model of argon used in earlier work. It is stable in the fcc lattice and we have been able to obtain its lattice vibrational structure and derived quantities such as the density of phonon states. The results agree in general form with others obtained for fcc lattices made up of atoms interacting via two-body central force potentials, but of, course, these do not show the high energy shoulder on the phonon distribution which derives from electronic effects. In addition, the values of the heat of formation and heat of activation for vacancies in this model at 0 K are known in terms of the well-depth parameter, ϕ_0 (Gillan and Finnis 1978). An important advantage of the model is that our results for the heat of transport can also be scaled in terms of ϕ_0. Now Cherns *et al* (1977) fixed this parameter by the cohesive energy of Au since their aim was to model sputtering experiments, whereas it has long been known that in metals such a procedure leads to overestimates of vacancy formation energies. In particular, with the value of ϕ_0 assigned by them (0.638 eV) the values for the vacancy formation and migration energies ($6\phi_0$ and $4.14\phi_0$ respectively) would be unreasonably large compared to the observed values. Since our results can be scaled to give the heat of transport as a ratio to ϕ_0 we can therefore fix ϕ_0 by the observed value of other more appropriate quantities, e.g. the vacancy migration energy (0.83 eV,[3] Flynn 1972) rather than the cohesive energy when we want absolute predictions.

The molecular dynamics method of our calculations uses a simulated microcanonical ensemble with constrained starting configurations corresponding to particular temperatures following the original scheme of Bennett (1975). This has been described in detail previously (Jones *et al* 1999). For a recent fundamental analysis of the method see Allnatt (2001). The computation proceeds by first obtaining the quantity (5) and then the heat of transport in the centre of mass frame from (7). Equivalently, since we are here dealing with a pure metal, the heat of transport of the vacancies is the negative of that for the atoms. These are of course classical mechanical calculations and although we can obtain results for temperatures less than the Debye temperature we cannot expect them to be valid there. The results reported here are thus all for temperatures greater than the Debye temperature, approximately 360 K, whether we use the Cherns *et al* parameters (360 K) or ours. (N.B. the experimentally determined melting temperature of gold is 1338 K, Emsley (1991).)

Some particular details should be noted. Firstly the motion of the jumping atom must be described relative to its surroundings in the lattice. This is done by introducing a 'reaction coordinate', commonly taken to be a linear function of the Cartesian coordinates of the hopping atom and of those four atoms which in the fcc lattice make up the 'gateway' through which the jumping atom must pass in order to get to the vacant site; see equation (3) of Jones *et al* (1999). We have made all the calculations described here with this choice, but tests of other choices indicate no significant differences in the results.

Secondly, we take the periodicity volume to be cubic and here we shall describe results for a periodicity volume including 108 lattice sites, of which the central site is vacant. Although relatively small it allows us to verify various details of the model accurately without excessive computer demands.

Thirdly, several temperatures were chosen in the range 300–1400 K. It should be noted, however, that the temperatures chosen for the initial constrained system will be lower than those of the corresponding final system because the excess potential energy associated with the constraint is distributed throughout the system as both potential and kinetic energy when the constraint is removed, the additional kinetic energy leading to a rise in temperature. When we specify temperatures in our results these are final temperatures in every case.

Fourthly, on average in the fcc lattice, vacancy movements occur in $\langle 110 \rangle$ directions by the jumps of neighbouring atoms into the vacant site as a result of thermal activation. Consequently for atom jumps in a particular [110] direction we expect the average associated heat current also to be in the [110] direction and the average heat current in the perpendicular, [001], direction to be zero. The heat current associated with any particular atomic jump is highly oscillatory as a function of time and it is necessary to take averages over very many jumps to obtain consistent results. Better averages and better constancy on the total energy and momentum (equal to zero) are obtained with smaller time steps. The time step used with the present results was 1 fs. We found that larger time steps gave notably less satisfactory results. Energy and momentum conservation were then good to one part in 10^5.

3. Heat currents and heat transfer

The two principal parts of our results are (i) the average heat current per thermally activated atom jump into a vacancy, $\overline{q}(t)$,

[3] We should stress that the experimental values quoted in this paper are probably not accurate to better than a few one-hundredths of an eV.

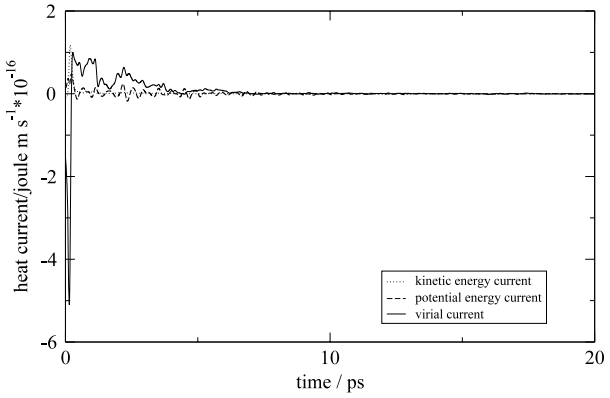

Figure 1. The three components of the heat of transport, at 600 K (averaged over 140 K trajectories).

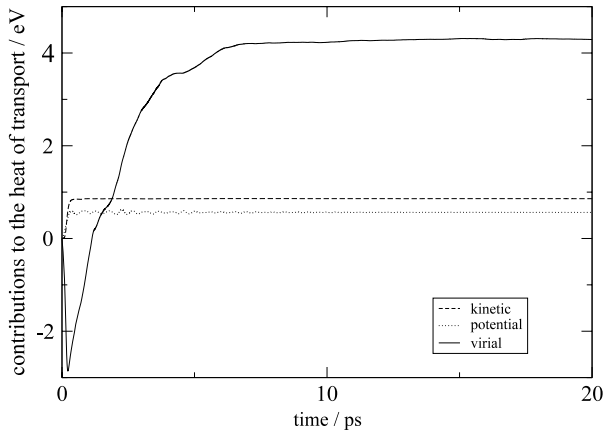

Figure 2. Kinetic, potential and virial contributions to the heat of transport at 600 K (averaged over 140 K trajectories).

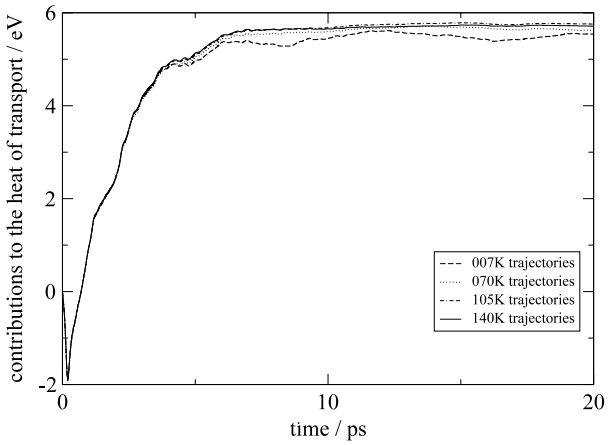

Figure 3. The variation of the heat of transport with number of trajectories, at 600 K.

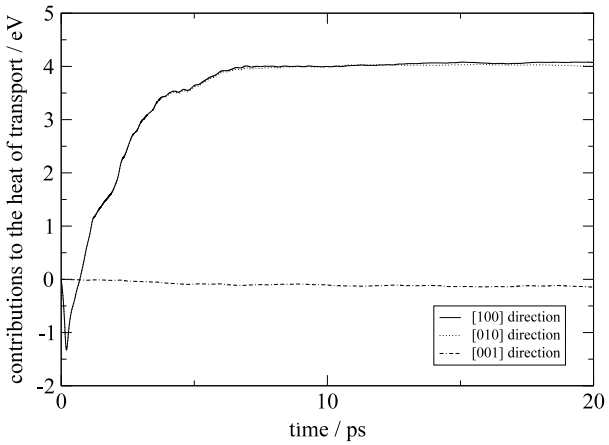

Figure 4. The contributions to the heat of transport from the heat currents in the [100], [010] and [001] directions (averaged over 140 K trajectories at 600 K).

and (ii) the time integral of this quantity, i.e. the average total heat transfer per atom jump which yields the heat of transport, $Q^*_{\rm G}$ by (7). We present results for a temperature of 600 K to illustrate the important features of the behaviour we have found.

Firstly, figure 1 for the average heat current $\overline{q}(t)$ shows the breakdown into the contributions from the three terms kinetic, potential and virial in the expression (5). It will be seen that the kinetic and potential contributions decay to zero quite quickly after reaching their maximum values whereas the virial contribution decays notably more slowly. This difference is reflected in their time integrals: the kinetic and potential parts reach asymptotic values within times of the order of 1 ps, whilst the virial part only does so after considerably longer (∼10 ps). This is shown in figure 2. The consequence is that the greater part of the time integral (7) comes from the virial term in (5).

This dominance of the virial term also appears when we look at the convergence of the average heat transfer as a function of the number of independent trajectories used to obtain these averages. Figure 3 shows this convergence up to 140 000 trajectories. It can be seen that this number is adequate to yield a well-defined limiting value at long times. However, averages taken over small numbers of trajectories do not give a sufficiently smooth long-time behaviour to allow an asymptotic value of the integral to be inferred—behaviour which again results from the dominance of the virial contribution. We earlier remarked on the expected spatial symmetry of the Cartesian components of the average $\langle \mathbf{J}_q \rangle$. Figure 4 shows that these expectations are confirmed. With the atomic jump direction as [110] we find that the average heat currents in the directions [100] and [010] are closely equal while that in the perpendicular direction [001] is close to zero. In other words the average heat flow in these simulations is overwhelmingly in the same direction as the atomic displacements. We emphasize that these features are only accurately confirmed when the averages are taken over many thousands of transitions.

To summarize these features:

(i) The major contributor to the average heat current and its time integral the heat transfer, comes from the virial term in (5).

(ii) Averages have to be taken over many thousands of atomic jumps to obtain smooth and consistent results for the heat transfer even for simulations corresponding to many tens of ps.

(iii) Fluctuations in the average heat transfer are greater when longer time steps are used in the routine for integrating the equations of motion in the m.d. simulation. We found that 1 fs was satisfactory but that with larger values, e.g. 5 fs, it was more difficult to obtain consistent results.

(iv) When the conditions for smooth and consistent results are met the expected spatial symmetry of $\langle \mathbf{J}_q \rangle$ is found.

(v) The conditions for smooth and consistent results depend upon circumstances; in particular they are more demanding at higher temperatures and less so at lower temperatures.

4. Comparison with experimental results

From the computational results like those presented in figures 1–4 we can obtain the predicted heats of transport. Experimental results on pure metals have mostly been obtained from measurements of the shift of markers fixed in the atomic lattice of specimens held in a temperature gradient (see e.g. Meechan and Lehman 1962, Jaffe and Shewmon 1964, Mock 1969). In these experiments the directly measured quantity on account of the gradient in vacancy concentration is $Q^{*\prime} - h_{\rm fv}$ where $Q^{*\prime}$ is the reduced heat of transport of the atoms and $h_{\rm fv}$ is the heat of formation of the vacancies, known from other experiments. Sometimes this combined quantity is called the *effective* heat of transport. When $h_{\rm fv}$ is taken to be 0.94 eV (Simmons and Balluffi 1962) the values of $Q^{*\prime}$ obtained from these experiments on Au range from 0.59 to 0.80 eV, reasonably consistent in view of the difficulty of these experiments. We emphasize that these are the reduced heat of transport for the Au atoms in the solid Au lattice.

Our computed results can be presented in several ways (table 1). Firstly we have the values of the expression (7) for the five temperatures of these computations. By the constraints imposed on the molecular dynamics these values correspond to motion of the Au atoms relative to the centre-of-mass of the system, whereas the experimental measures correspond to motion relative to the crystal lattice. The quantities obtained from (7) must therefore be corrected as follows

$$Q_l^* = Q_{\rm G}^* + u,$$

where, in this constant volume system, u is the internal energy per atom, equal to $-6\phi_0$ in this bond model solid (see, for example, Jones *et al* 1997). (In a constant pressure system the addition would be the enthalpy per atom, h.) However, to obtain the *reduced* heat of transport per atom from Q_l^* we must subtract u (h in a constant pressure system) cf (3). The end result is thus that we should compare $Q_{\rm G}^*$ directly with the measured reduced heat of transport, $Q^{*\prime}$. This can be done from the values given in column 2 of table 1, from which it will be seen that the computed quantities are considerably larger than the experimental values, which range from 0.59 to 0.78 eV in the temperature range 1200–1300 K. The reason for this we believe lies in the fact that the potential model of Cherns *et al* (1977) specified in the appendix has been fitted to the cohesive energy of gold. Now it is well known that pair potentials fitted to the cohesive energy of metals generally overestimate vacancy formation energies and associated defect quantities (see, for example, (Finnis and Sinclair 1984)). In the present case fitting the model to the cohesive energy of gold has thus overestimated the well-depth parameter ϕ_0.

Table 1. The second column gives the reduced heat of transport $Q^*(=Q_{\rm G}^*)$ in eV as obtained from equation (7) with the use of the data in table A.1. The experimental values range from 0.59 eV (Jaffe and Shewmon 1964) to 0.80 eV (Mock 1969). Column 3 gives the ratio $Q_{\rm G}^*/h_{\rm mv}$ for our potential model, whilst the last column gives the reduced heat of transport obtained from the calculate values in the third column together with the experimental value of $h_{\rm mv}$ (0.83 eV, Flynn 1972).

T (K)	$(Q_{\rm G}^*/eV)_1$	$(Q_{\rm G}^*/h_{\rm mv})$	$(Q_{\rm G}^*/eV)_2$
370	9.3	3.5	2.9
600	5.8	2.2	1.8
730	3.9	1.5	1.2
1100	2.0	0.77	0.64
1440	1.2	0.46	0.38

However, it is not difficult to show that all the basic equations of the present computations can be put into a dimensionless form by introducing the scaled variables for mass ($=m/m_{\rm Au}$), distance ($=r/r_0$) and energy ($=E/\phi_0$), with corresponding scaled quantities for time, velocity, etc. Since the mass of all atoms in these computations is the same and equal to $m_{\rm Au}$ and the nearest neighbour distance $s(=r_0)$ is also a constant it follows that $Q_{\rm G}^*$, being an energy, scales as ϕ_0, i.e. that $Q_{\rm G}^*/\phi_0$ depends only on temperature. Thus if ϕ_0 is overestimated so is $Q_{\rm G}^*$.

Now simple theories of the heat of transport have often related it to the heat of activation of the vacancies $h_{\rm mv}$, which for this model is known to be $4.14\phi_0$ (Gillan and Finnis 1978). Column 3 in table 1 therefore shows the calculated ratios $Q_{\rm G}^*/h_{\rm mv}$, which is likewise independent of ϕ_0. The experimental values for this ratio range from 0.63 (Jaffe and Shewmon 1964) to 0.96 (Mock 1969). This comparison is much more meaningful and it shows that there is fair agreement with the measured ratios at the temperatures of their experiments which were conducted at 1200–1300 K.

If we now use the experimental value of $h_{\rm mv}$ (0.83 eV Mock 1969) to convert these predicted ratios of $Q_{\rm G}^*/h_{\rm mv}$ to values of $Q_{\rm G}^*$ we obtain the values given in column 4 of table 1. This is equivalent to choosing ϕ_0 to give the correct values of the vacancy migration energy ($\phi_0 = 0.2eV$). It will be seen that the values of $Q_{\rm G}^*$ in column 4 arrived at in this way are in fair agreement with the values obtained experimentally. We conclude therefore that reasonable values of the heat of transport for defects in metals may be obtained with the method we have used in conjunction with pair potentials when these are fitted to defect energies rather than cohesive energies.

Table 1 shows that our results predict a distinct decrease of $Q_{\rm G}^*$, i.e. of the reduced heat of transport, with increasing temperature. In figure 5 we plot $Q_{\rm G}^*$ against inverse temperature. In fact the values of $Q_{\rm G}^*$, in column four, as is shown in figure 5, closely follow a linear function of the inverse temperature over the range studied and this function is given by

$$\left(Q_{\rm G}^*/eV\right) = 1.27\,(1000/T/K) - 0.49. \qquad (8)$$

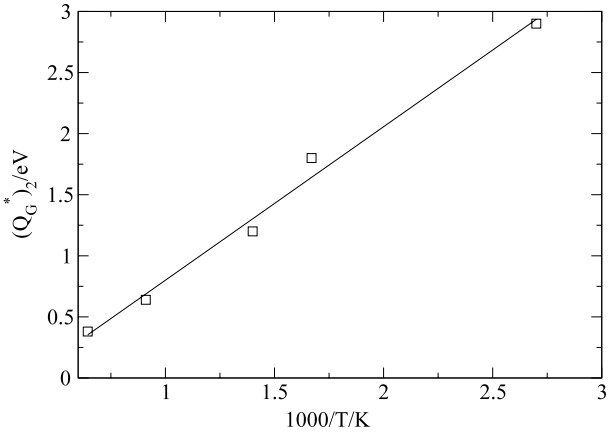

Figure 5. $(Q_G^*\ \mathrm{eV}^{-1})_2$ plotted against $1000/T$.

The greater part of this variation with temperature derives from the virial term in the average heat current (7) and reflects the temperature sensitivity of its decay with time. By contrast, the kinetic energy and potential contribution to Q_G^* are both largely independent of temperature, a consequence of the rapid decay of the corresponding parts of the average heat current. These characteristics are similar to those found previously in the studies of solid Ar and similar explanations apply here as were presented by Jones *et al* (1999).

5. Conclusions

In this work we have explored two aspects of the calculation of the heat of transport of defects in crystalline solids, the first technical and the second physical implications. The first concerns some technical aspects of the constrained molecular dynamics method devised for simulating rare atomic movements in solids (Bennett 1975). In the present case we have used it to calculate the heat of transport of vacancy defects in a model fcc solid. In particular, we have examined the size of time step and the number of atom movements needed to obtain clear and accurate results. Since the method involves a two-stage computation, namely the preparation of an ensemble of constrained configurations and the following unconstrained dynamical calculation following passage of the atom over the saddle point into the vacancy, it does not seem possible to estimate the necessary time step and necessary number of trajectories on the basis of previous experience with more usual molecular dynamics calculations. We have therefore had to proceed more empirically. We have judged the quality of our results (a) by the conformity of the average heat flux to the expected spatial symmetry and (b) by the approach of the integrated heat flux to its asymptotic value at long times after the atom crosses the saddle point. For our system we found that it was necessary to use a time step of 1 fs with averages over some 100 000 atomic trajectories to obtain satisfactory results for the heat of transport at elevated temperatures. We have found no evidence that the requirements would be significantly less severe in other systems. By these means we have obtained accuracies significantly greater than that of any previous calculations of the heat of transport by the present or other methods.

As to the physical implications, the decrease of the reduced heat of transport with rising temperature is a definite prediction of this work. Furthermore, the predicted ratios of the reduced heat of transport to the activation energy for vacancy migration at high temperatures for model Au match the magnitude of the same ratio determined experimentally in the same temperature range. Indeed our results go someway to explaining the difference between the results of different workers when the different temperature ranges of their experiments are taken into account. Lastly we have also shown that when the parameter ϕ_0 in the potential model is scaled by reference to the activation energy of vacancy migration then the predicted absolute values of $Q^{*'}$ are close to the experimental measures.

Table A.1. Potential and simulation data (Cherns *et al* 1977).

m_{Au} (kg)	3.27×10^{-25}
r_0 (m)	2.88×10^{-10}
ϕ_0 (eV)	0.638
α (m^{-1})	1.581×10^{-10}

Acknowledgments

The authors gratefully acknowledge the benefit of discussions and correspondence with Professor A R Allnatt.

Appendix. The interatomic potential

The form of the potential function and the parameters employed were taken from Cherns *et al* (1977). namely

$$\phi(r) = \begin{cases} \phi_0 \{\exp[-2\alpha(r-r_0)] - 2\exp[-\alpha(r-r_0)]\}; \\ \qquad r < r_0 \\ -\phi_0 + \frac{1}{2}\gamma(r-r_0)^2 + \frac{1}{6}\delta(r-r_0)^3; \\ \qquad r_0 < r < r_1 \\ 0; \qquad r_1 < r \end{cases}$$

with $\alpha r_0 = 4.55$. The function is continuous with continuous first derivatives at r_0. The constants γ, δ and r_1 are chosen (i) so that the second derivative of ϕ is also continuous at r_0 and (ii) ϕ and its first derivative are both zero at $r_1 (> r_0)$ which gives

$$r_1 = r_0 + \frac{\sqrt{3}}{\alpha}$$

$$\gamma = 2\alpha^2\phi_0$$

$$\delta = \frac{4}{\sqrt{3}}\alpha^3\phi_0$$

and the parameters are collected together in table A.1.

However it should be noted that it is convenient to introduce the dimensionless energy variable $E'(\equiv E/\phi_0)$, and distance variable $r'(\equiv r/r_0)$ with the additional mass variable $m'(\equiv m/m_{\mathrm{Au}})$ from which the dimensionless time

$t'(=(\phi_0/mr_0^2)^{1/2}t)$ and velocity $v'(=(m/\phi_0)^{1/2}v)$ can be derived. It is simple to show that all the relevant equations have the same form in reduced units as in physical units.

References

Allnatt A R 2001 *J. Phys. A: Math. Gen.* **34** 7441
Allnatt A R and Chadwick A V 1967 *Chem. Rev.* **67** 681
Allnatt A R and Lidiard A B 1993 *Atomic Transport in Solids* (Cambridge: Cambridge University Press)
Becker K G and Hoheisel C 1982 *J. Chem Phys.* **77** 5108
Bennett C H 1975 *Diffusion in Solids—Recent Developments* ed A S Nowick and J J Burton (New York: Academic) pp 74–113
Born M and Huang K 1954 *The Dynamical Theory of Crystal Lattices* (Oxford: Clarendon)
Cherns D, Finnis M W and Matthews M D 1977 *Phil. Mag.* **35** 693
Doan N V 1988 *Phil. Mag.* A **58** 179–92 (see also other papers in the same issue No.1 July 1988)
Emsley J 1991 *The Elements* 2nd edn (Oxford: Clarendon)
Finnis M W and Sinclair J E 1984 *Phil. Mag.* A **50** 45
Flynn C P 1972 *Point Defects and Diffusion* (Oxford: Clarendon)
Gerl M 1967 *J. Phys. Chem. Solids* **28** 725
Gillan M J 1977 *J. Phys. C: Solid State Phys.* **10** 1641–57
Gillan M J 1983 *Mass Transport in Solids* ed F Benière and C R A Catlow (New York: Plenum) pp 227–50
Gillan M J and Finnis M W 1978 *J. Phys. C: Solid State Phys.* **11** 4459–83
Gillan M J, Harding J H and Tarento R-J 1987 *J. Phys. C: Solid State Phys.* **20** 2331–46
Harding J H 1990 *Rep. Prog. Phys.* **53** 1403–66
Hoheisel C and Vogelsang R 1988 *Comput. Phys. Rep.* **8** 1–69
Irving J H and Kirkwood J G 1950 *J. Chem. Phys.* **18** 817–29
Jaffe D and Shewmon P G 1964 *Acta Metall.* **12** 515–27
Janek J, Korte C and Lidiard A B 2002 *Thermal Non-Equilibrium Phenomena in Fluid Mixtures* (*Springer Lecture Notes in Physics* vol 584) (Berlin: Springer) pp 146–83
Jones C, Grout P J and Lidiard A B 1996 *Phil. Mag. Lett.* **74** 217–23
Jones C, Grout P J and Lidiard A B 1997 *Ber. Bunsenges. Phys. Chem.* **101** 1232–7
Jones C, Grout P J and Lidiard A B 1999 *Phil. Mag.* **79** 2051–70
Meechan C J and Lehman G W 1962 *J. Appl. Phys.* **33** 634–41
Mock W 1969 *Phys. Rev.* **179** 663
Philibert J 1991 *Atom Movements Diffusion and Mass Transport in Solids* (Les Ulis: Editions de Physique)
Shewmon P 1989 *Diffusion in Solids* (Pennsylvania: Minerals, Metals and Materials Society)
Simmons R O and Balluffi R W 1962 *Phys. Rev.* **125** 862
Vogelsang R and Hoheisel C 1986 *Z. Naturf.* a **41** 1051
Vogelsang R and Hoheisel C 1987a *J. Phys. C: Solid State Phys.* **20** 5923–32
Vogelsang R and Hoheisel C 1987b *J. Phys. C: Solid State Phys.* **20** 5933
Wever H, Frohberg G and Adam P 1973 *Elektro- und Thermo-Transport in Metallen* (Leipzig: Barth)